

THE NGC 1399 GLOBULAR CLUSTER SYSTEM

Doug Geisler

National Optical Astronomy Observatories^a
Cerro Tololo Inter-american Observatory

Juan Carlos Forte

Instituto de Astronomía y Física del Espacio

RESUMEN. Se obtiene con un CCD en el foco primario del telescopio de 4-m de Cerro Tololo fotometría integrada en el sistema de Washington para el complejo de cúmulos globulares de NGC 1399. Se alcanza $V \sim 24.5$ y se incluyen ~ 2000 cúmulos. Luego de corregirse los datos incompletos, los efectos del fondo y los errores sistemáticos de la fotometría, la función de luminosidad resultante muestra un máximo en $T_1 = 23.0 \pm 0.15$ ó sea $V = 23.45 \pm 0.16$. Si la magnitud absoluta correspondiente es igual a la del sistema de cúmulos globulares galácticos, el módulo de distancia de Fornax es 30.95 ± 0.22 ó sea 0.7 menos de lo que se encuentra para Virgo con idéntico método. Se obtiene para la constante de Hubble 68 ± 13 si se asume el valor usual de la velocidad hacia Virgo del Grupo Local. Alternativamente se estima para esa velocidad 365 km s^{-1} .

Se obtienen abundancias para ~ 100 cúmulos usándose un índice libre de enrojecimiento. En promedio los cúmulos muestran $[\text{Fe}/\text{H}] = -1.0$ pero con distribución extendida y llana. Una fracción apreciable de cúmulos tiene abundancias que aparentemente exceden la del sol.

ABSTRACT. Integrated Washington photometry has been obtained for the globular cluster system of NGC 1399 with the CTIO 4-m prime focus CCD. The data extend to $V \sim 24.5$ and include ~ 2000 clusters. After corrections for incompleteness, background and systematic photometric error, the derived luminosity function clearly shows a turnover at $T_1 = 23.0 \pm 0.15$, or $V = 23.45 \pm 0.16$. Assuming the absolute magnitude of this peak is the same as for the Galactic globular cluster system yields a distance modulus of 30.95 ± 0.22 for Fornax, or 0.7 mag closer than found for Virgo using the same method. A Hubble constant of 68 ± 13 is derived assuming a canonical value for the Local Group Virgocentric infall velocity. Alternatively, solving for this infall velocity gives a value of 365 km s^{-1} .

Abundances are also derived for ~ 100 clusters from the system's integrated, reddening-free abundance index. The clusters have a mean metallicity of $[\text{Fe}/\text{H}] = -1.0$ with a broad, flattened abundance distribution. A significant fraction of the clusters have an abundance apparently exceeding the sun's.

Key words: CLUSTERS-GLOBULAR

I. INTRODUCTION.

Globular cluster systems (GCSs) offer unique opportunities to investigate the oldest stellar components of galaxies. Evidence is becoming increasingly favorable for their use as accurate distance indicators as well. The recent study by Harris (1989) is particularly

a) Cerro Tololo Inter-American Observatory, National Optical Astronomy Observatories are operated by the Association of Universities for Research in Astronomy, Inc., under contract with the National Science Foundation.

convincing in this regard: he presents the results of an extensive CCD survey of the GCSs associated with 4 elliptical galaxies in the Virgo cluster, including the "anomalous" M87 system, and demonstrates that all 4 luminosity functions (LFs) have the same turnover, to within 0.25 mag, and the same gaussian shape. Hanes and Whittaker (1987) have recently argued that one can obtain a distance estimate accurate to 15% using globular cluster LFs, even when the data fail to reach the turnover luminosity by as much as 1 mag.

The NGC 1399 GCS is a particularly interesting one. This galaxy is the central, dominant elliptical galaxy in the Fornax cluster. Such galaxies are found to have the most populous GCSs known (Harris and Smith 1976, Harris, Smith and Myra 1983). Dawe and Dickens (1976) first detected the NGC 1399 GCS. Hanes and Harris (1986) followed this with a more extensive photographic study, where they showed that the NGC 1399 GCS was indeed very populous, with perhaps the highest specific frequency (ratio of total globular cluster population to the luminosity of the parent galaxy) of any galaxy known. Given its proximity (radial velocity ~ 1250 km/s), the NGC 1399 GCS thus provides a very large sample of nearby clusters - indeed, the largest sample observable to $V \sim 24$ in the South. Moreover, since Fornax is in the Local Supercluster anticenter direction, a relative Fornax-Virgo distance determination yields a direct measurement of the Local Group infall velocity.

We have thus undertaken an investigation of the NGC 1399 GCS. Preliminary results are presented here - a final, more complete analysis will be published separately.

II. OBSERVATIONS

NGC 1399 was observed on 3 nights in December 1987 with the CTIO 4m RCA #1 prime focus CCD system. The nights were of excellent photometric quality. Data were obtained for a $3' \times 5'$ field centered on the galaxy, plus 3 surrounding frames and a background field located some 2° north of the galaxy. The seeing varied from 1.1-1.6". For the deep, central frames from which the LF was derived, the seeing was 1.2". Results are presented here only for the central field.

Data were obtained on the Washington photometric system. This system was chosen because of its broad bands (≥ 1000 Å), allowing deep LF data to be obtained, and because of its ability to derive accurate abundances efficiently (Canterna 1976). The integrated Washington abundance index, Q_{CMT} , for galactic globulars (Harris and Canterna 1977) correlates very well with other abundance indicators, e.g. integrated spectral type (Hesser and Shawl 1985) and Q_{39} (Zinn 1980). In addition, Q_{CMT} is virtually reddening-free, a problem that plagues abundance estimates based on integrated UBVRI photometry (Reed, Hesser and Shawl 1988), and has little or no sensitivity to horizontal branch morphology. For the central field, exposures totalling 2700s in C, 1800s in M, and 3600s in T_1 were obtained.

III. REDUCTIONS

The central field shows a strong gradient in the background galaxy light which can severely compromise photometric accuracy. Therefore, it is important to remove this background light as carefully as possible. We accomplished this satisfactorily using various IRAF routines. The stars were first removed by heavy smoothing and median filtering. The resulting image, containing only the galaxy light, was then subtracted from the original picture. The final image is mostly free from galaxy light, except in the center where the original frame was saturated.

Photometry of the stellar images was performed on the subtracted image using a version of the DAOPHOT program (Stetson 1987) provided by C. Pritchet. The sky measurements were taken from the smoothed, galaxy-only frame. The ALLSTAR routine was used to obtain the photometry. Note that NGC 1399 is sufficiently distant that its globular clusters appear stellar, so that a point-spread function fitting routine such as ALLSTAR is appropriate. Photometry for the background field was performed in the same manner.

The instrumental photometry was then transformed to the standard Washington system by means of aperture photometry derived for a large number of standards taken from Harris and Canterna

(1979) and Geisler (1989 in preparation). For the night on which the data were obtained for the central NGC 1399 field, 34 standard star observations were made. The rms residuals for the transformation to the standard system was 0.027 in C-M, 0.008 in M- T_1 , and 0.013 in T_1 .

In order to investigate the effects of crowding and incompleteness and to better determine the errors (random and systematic) as a function of magnitude, artificial stars were generated with the ADDSTAR routine, inserted into the galaxy background-subtracted central T_1 frame, and the frame re-reduced in exactly the same manner as before. Twenty stars were added in each of 10 separate trials at a variety of magnitudes, ranging from the brightest to the faintest clusters observed, and the results analyzed with a program kindly supplied by C. Pritchett.

IV. THE LUMINOSITY FUNCTION

The T_1 vs. M- T_1 color-magnitude diagram for the central field is shown in Figure 1, and that for the background field in Figure 2. The strong enhancement of objects in the central frame with intermediate colors over the background is obvious. In particular, there are only 4 objects in the background field with $0.5 < M-T_1 < 1$ brighter than $T_1 = 22$, while 183 are found in the galaxy frame. The lines in Figure 1 delimit the region which we will consider the globular clusters to inhabit. Clearly, based on a comparison of Figures 1 and 2, there are a large number of globular clusters present. The DAOPHOT FIND routine encountered some 1300 objects in the central frame. Of these, ~100 are galaxies, multiple detections on saturated images or bad columns, etc., while ~200 objects were found in the background field. Thus, there are ~1000 clusters in the central frame, or more than 3/4 of the objects found.

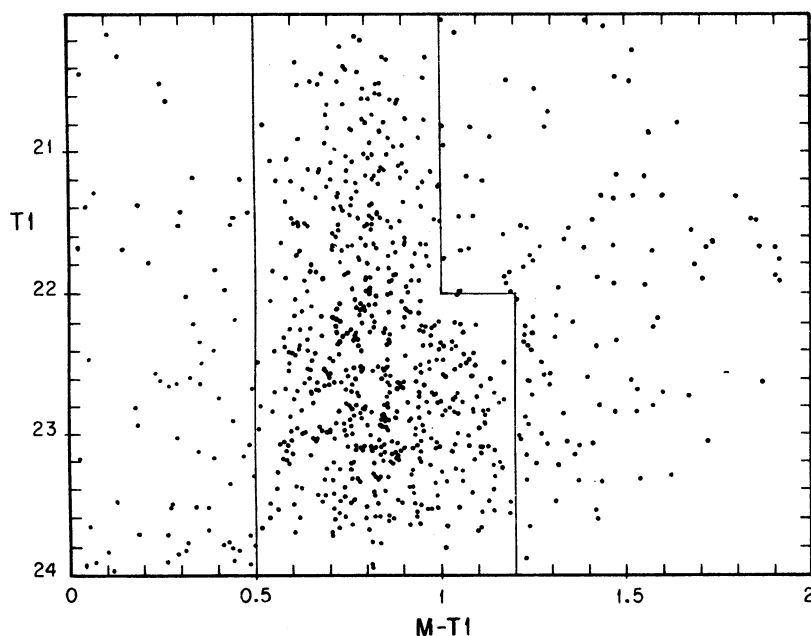


FIG. 1.- T_1 vs. M- T_1 color-magnitude diagram for the central NGC 1399 field. The lines demarcate the strong globular cluster sequence.

The first step in deriving a LF is to simply count the number of objects within the defined region in Figure 1 in different magnitude bins. This "raw" LF is shown in Figure 3. Note that the limit of the photometry is $T_1 \sim 23.8$. For a typical globular cluster, this is equivalent to $V \sim 24.3$ or $B \sim 24.9$. Note also the apparent turnover near $T_1 \lesssim 23$.

However, Figure 3 must be corrected for several effects before an accurate LF is achieved. First, one must determine if there are any systematic errors in the photometry, and if so,

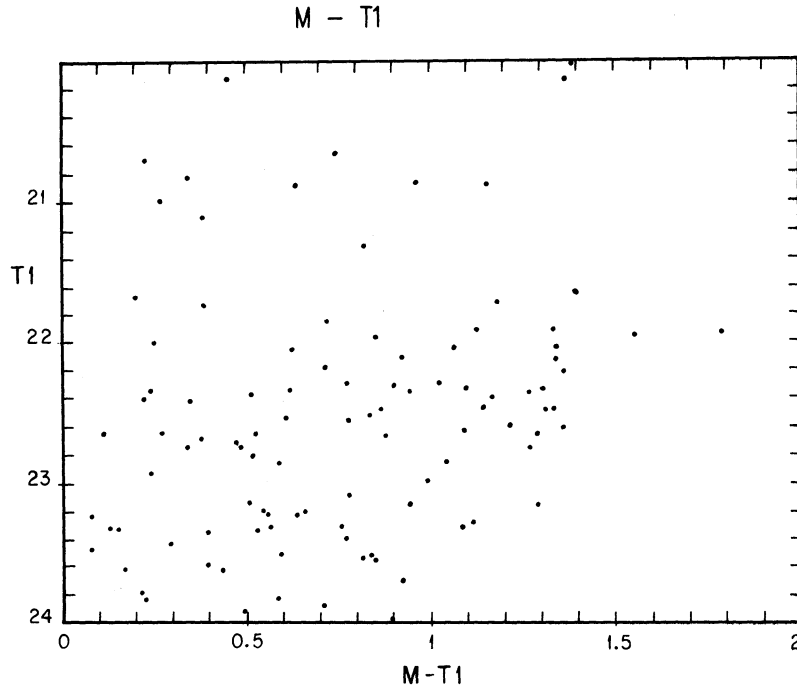


FIG. 2.- Same as Figure 1 for the background region.

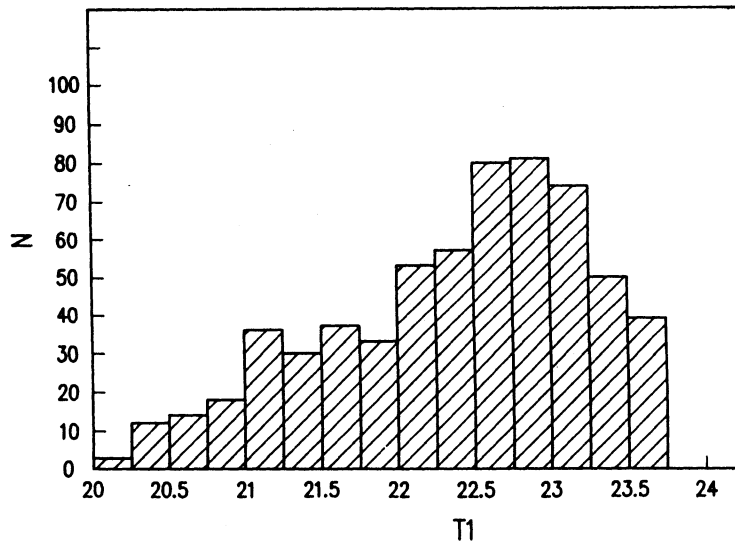


FIG. 3.- The "raw" luminosity function for the NGC 1399 globular cluster system.

correct the magnitudes accordingly. Secondly, crowding and photon statistics cause the FIND routine to recover an increasingly smaller fraction of the true number of objects at fainter magnitudes. One must then multiply the number of objects found by this incompleteness factor, which varies dramatically with magnitude. Finally, the number of background objects must be subtracted.

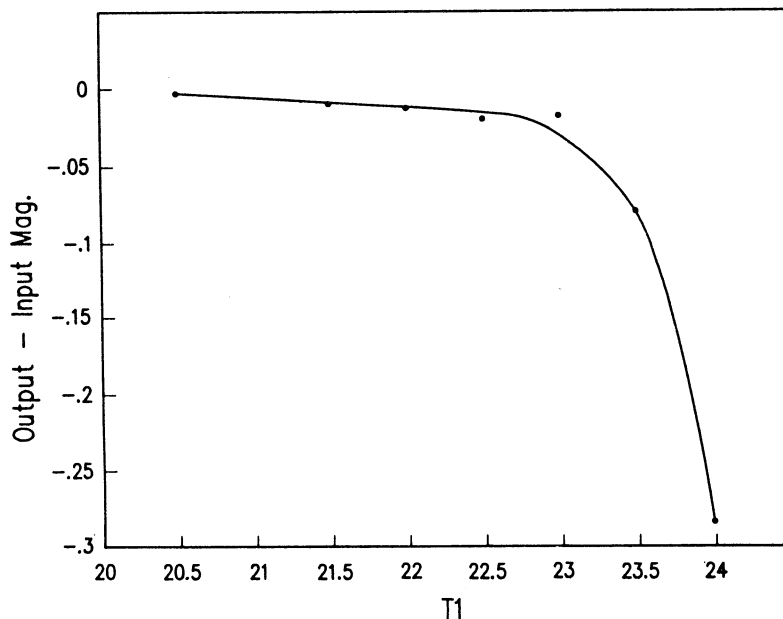


FIG. 4.- Output- input magnitude vs. input magnitude from the ADDSTAR experiments. Each point represents the mean for a sample of 200 artificial stars.

Figures 4 and 5 show the results of the ADDSTAR experiments to derive the systematic photometric errors and the completeness corrections. The input magnitude is the magnitude of the added star and the output magnitude is the value returned by ALLSTAR. Note that the program consistently finds objects to be brighter than they really are, but the error is not significant until fainter than $T_1 \sim 23$. At the magnitude of the "turnover" ($T_1 \sim 23$), the effect is ≤ 0.03 mag. Similarly, incompleteness does not become important until beyond this level. At $T_1 = 23$, 93% of the objects are recovered, but this number falls to 50% at $T_1 \sim 23.75$. Data fainter than this will not be considered in deriving the LF, as the corrections are large and uncertain. Note that this is ~ 0.75 mag beyond the "turnover".

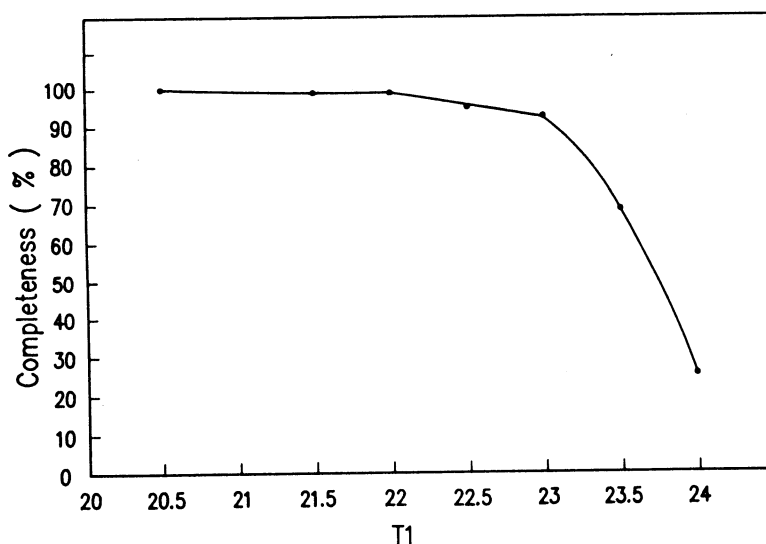


FIG. 5.- Percentage of added stars found as a function of input magnitude. Each point is determined from 200 artificial stars.

The false star results also indicate that the random errors are ~ 0.15 at $T_1 \sim 23$. In addition, the background contamination at this magnitude is $\sim 11\%$.

We can now correct our raw LF for the above effects and derive Figure 6. Interestingly, Figure 6 is remarkably similar to Figure 3. This is because all of the effects are very small brighter than 23, and fainter than this, the competing effects of incompleteness and background contamination, though large, tend to cancel each other out. However, we can now be confident that the turnover near $T_1 \sim 22.8$ is real, and that our incompleteness limit of 23.75 is almost 1 magnitude beyond the turnover.

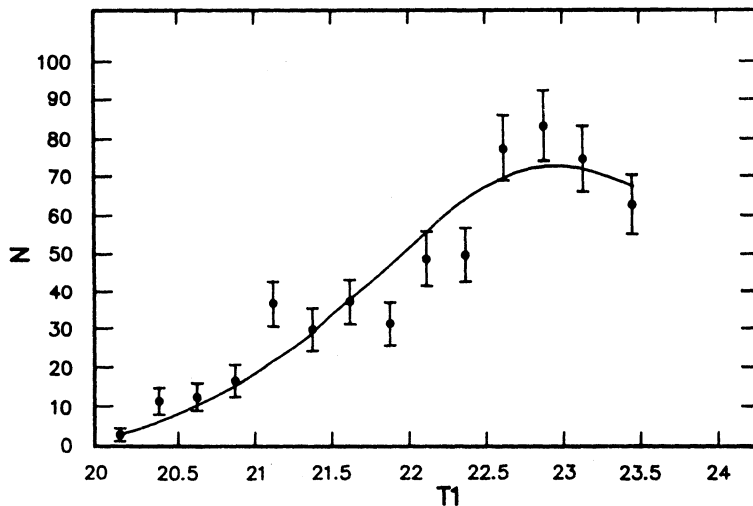


FIG. 6.- The corrected luminosity function. Root N error bars are shown. The curve is a gaussian with $\sigma = 1.2$ and peak magnitude = 23.0.

V. DISTANCE DETERMINATION

Now that we have the corrected LF for the globular clusters in NGC 1399, how do we use it to derive a distance? The idea is simple: fit the NGC 1399 LF to that of a GCS whose distance is known. Given that: 1) the two LFs have the same characteristics, i.e. the same absolute magnitude at the turnover and the same gaussian shape; and 2) the distance to the comparison GCS is known to high accuracy, this method is a very straightforward and powerful one, and avoids any intermediate steps. If one uses the Galaxy's GCS as the comparison, as we do, it is then a single step from our Galaxy to any other galaxy. As the peak (turnover) magnitude is relatively bright ($M_b = -7.6$), the method is applicable to distances as large as 60 Mpc, or about 3 times farther than the Virgo cluster (Harris 1989). Ultimately, we must rely on the RR Lyrae distance scale, which still has uncertainties at about the 0.2 mag level (Barnes and Hawley 1986, Jones *et al.* 1987).

The key assumption is that different GCS have the same properties. Although there is still no satisfactory theoretical explanation for this, observational support is mounting rapidly. As Harris (1987) has demonstrated, the GCSs in galaxies as different as M87 and the Fornax dwarf spheroidal, although differing by orders of magnitude, have mean or peak luminosities that are the same to within the errors. Even more convincing support is provided by Harris' (1989) recent CCD data for 4 E galaxies in Virgo. It is reasonable to suspect that a GCS as anomalous as that of M87 in terms of sheer numbers of clusters may also be expected to be anomalous in its other properties, specifically turnover luminosity and/or gaussian width (σ). However, Harris' data show that the turnovers for 3 other, normal ellipticals in Virgo coincide with that of M87 within the errors, as do the σ values. Thus, GCS are becoming increasingly attractive distance indicators. However, as the GCS of the Galaxy (a spiral) is often used as

the fiducial one to compare with those of E galaxies, it remains to show that the LFs of a spiral and elliptical galaxy in the same cluster have the same turnover and σ . Although difficult observationally, given the relatively poor GCSs of spirals, this problem is now under attack.

To proceed with the distance determination, we first fit a gaussian function to our LF assuming $\sigma = 1.2$ (our data yield $\sigma = 1.2 \pm 0.2$) and $(M_V)_{\text{peak}} = -7.6 \pm 0.15$ - appropriate values for the Galaxy's GCS (Harris 1989). Our preliminary best fit is shown in Figure 6, with a peak magnitude of $T_1 = 23.0 \pm 0.15$, or $V = 23.45 \pm 0.16$. The visual distance modulus is then $(m-M)_V = 31.05 \pm 0.22$. Assuming a reddening of ≤ 0.03 (Hanes and Harris 1986), and $R = 3.2$, the true distance modulus is $(m-M)_0 = 30.95 \pm 0.22$, or 15.5 ± 1.6 Mpc. Note that the error is only 10%. Under the same assumptions and procedure, Harris (1989) derives a modulus of 31.7 ± 0.22 for Virgo, i.e. 21.9 ± 2.2 Mpc.

The ratio of the distances to the Fornax and Virgo clusters derived for globular cluster LFs is then 0.71. This value is somewhat smaller than other recent determinations. Caldwell and Bothun (1987) find 0.8 from a comparison of the LFs of the dwarf elliptical galaxies; Dressler, *et al.* (1987) derive 1.1 from the $D_n: \sigma$ relation; and Ferguson and Sandage (1988) argue for a ratio of 1.0 from the LFs of a large sample of galaxies in the clusters.

Given the distance to the Fornax cluster and its radial velocity (1261 ± 50 km s⁻¹ - Dressler *et al.* 1987), we can immediately solve for the Hubble constant, after correcting for the infall velocity of the Local Group to the Virgo cluster (303 ± 39 km s⁻¹ - Aaronson *et al.* 1982). A value of 68 ± 13 km s⁻¹ Mpc⁻¹ is obtained, in good agreement with the value of 61 ± 7 which Harris (1989) derives from the GCSs in Virgo. Alternatively, we can derive the Virgocentric infall velocity of the Local Group, assuming the Harris (1989) distance to Virgo, and assuming that Fornax does not participate in this flow. We find 365 km s⁻¹ for the infall velocity and a Hubble constant of 66 km s⁻¹ Mpc⁻¹.

VI. CLUSTER ABUNDANCES

Harris and Canterna (1977) have shown that the integrated Washington colors of Galactic globular clusters can be combined to form a reddening-free index, Q_{CMT} (analogous to van den Bergh's (1967) Q index from integrated UBV photometry), which is a useful metallicity indicator. It is indeed more reddening-free than the UBV index. Hesser and Shawl (1985) find that Q_{CMT} is well-correlated with their integrated spectral types, and a plot of Q_{CMT} vs. $[\text{Fe}/\text{H}]$ from Zinn (1985) shows a spread no larger than expected from the respective errors (D. Geisler and M. Lee, private communication).

The Washington two-color plot for the NGC 1399 globulars is shown in Figure 7. Here we have displayed only objects brighter than $T_1 = 22$ with the best photometry. Fiducial lines for $[\text{Fe}/\text{H}] = 0, -1, -2$ and -2.5 are also given. These are derived from a calibration of Q_{CMT} with the Zinn (1985) Galactic globular cluster metal abundance scale. It is likely that the most deviant points in Figure 7 are unresolved galaxies. Also, the photometric errors are rather large, as shown.

In general, the globulars in NGC 1399 cover a range of metallicities similar to those in the Galaxy, except for a significant number at abundances exceeding solar. The abundances derived for these clusters are especially uncertain, however, as it requires an extrapolation of the calibration, since there are no globulars in the Galaxy more metal-rich than $[\text{Fe}/\text{H}] \sim -0.3$ (with one possible exception - see Armandroff and Zinn 1988). In any case, NGC 1399 does appear to contain clusters more metal-rich than does the Galaxy. This is not unexpected, as NGC 1399 contains an order of magnitude more clusters.

The abundance distributions for the globular clusters in NGC 1399 and the Galaxy are compared in Figure 8. Abundances for globulars in the Galaxy are from Zinn (1985) and Armandroff and Zinn (1988). The NGC 1399 distribution is much broader. This is due to two principal factors: 1). the photometric errors lead to a typical abundance uncertainty of ~ 0.5 dex; and 2). the Galaxy distribution is intrinsically bimodal, with halo and disk subsystems (Zinn 1985). Although the abundance errors in our study are large, a large number (97) of clusters has been investigated.

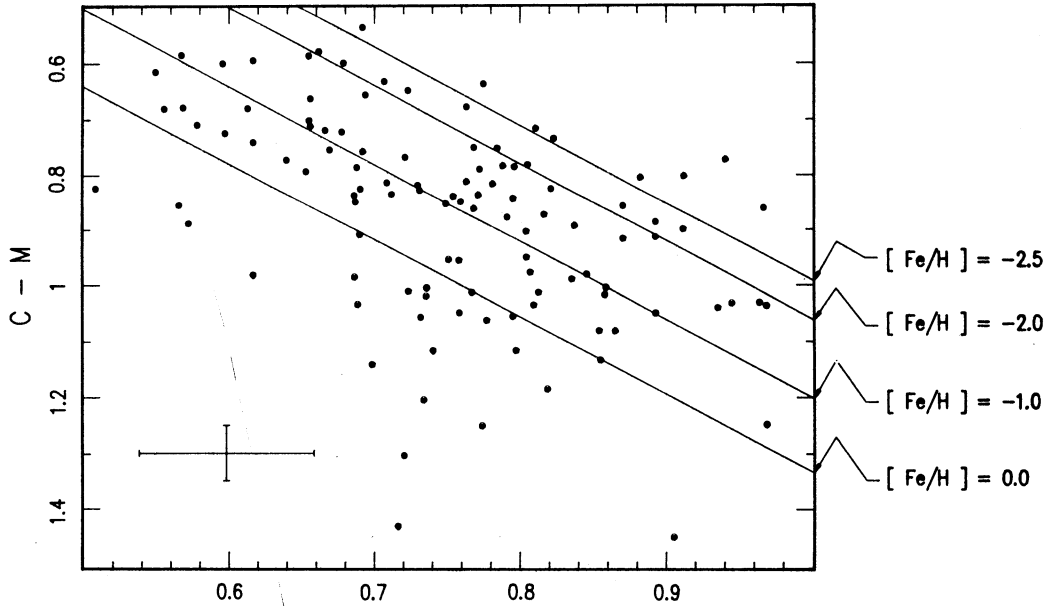


FIG. 7.- The C-M vs. $M-T_1$ two-color plot for bright globular clusters in NGC 1399. Fiducial abundance lines are given.

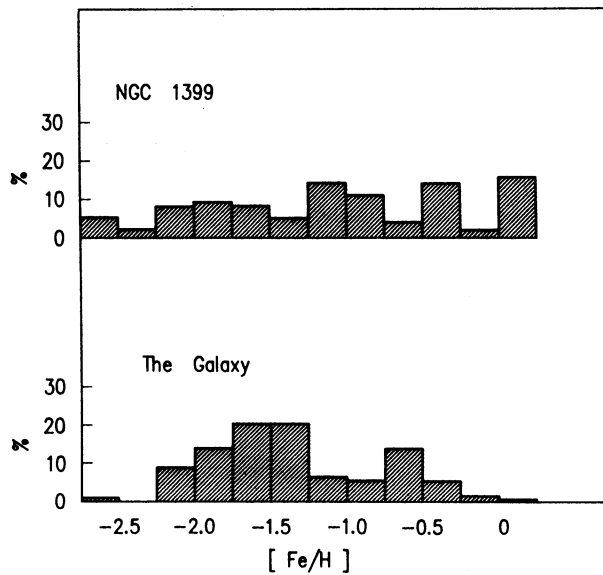


FIG. 8.- A comparison of the NGC 1399 and Milky Way globular cluster metal abundance distributions.

Finally, we can compare the mean metallicity of the globular clusters in different galaxies. For the 97 clusters in our sample, we obtain $\langle [\text{Fe}/\text{H}] \rangle = -1.01 \pm 0.1$. For the 123 Milky Way clusters in the sample of Zinn (1985) and Armandroff and Zinn (1988), the mean is -1.32 ± 0.05 . The largest sample of globular clusters in M87 with well-determined abundances is that of Mould, Oke and Nemec (1987), who derive -1.2 ± 0.2 from spectra of 27 clusters. The NGC 1399 system is then quite comparable in mean abundance to that of M87.

In the near future, we will add the data for the 3 other NGC 1399 fields. This should approximately double our sample of clusters.

We would like to acknowledge the help and advice of Dr. Chris Pritchett, especially for providing his computer program.

REFERENCES

- Aaronson, M., Huchra, J., Mould, J., Schechter, P.L., and Tully, R.B. 1982, Ap. J., 258, 64.
 Armandroff, T.E., and Zinn, R. 1988, A. J., 96, 92.
 Barnes, T.G., and Hawley, S.L. 1986, Ap. J. Lett., 307, L9.
 Caldwell, N., and Bothun, G.D. 1987, A. J., 94, 1126.
 Canterna, R. 1976, A. J., 81, 228.
 Dawe, J.A., and Dickens, R.J. 1976, Nature, 263, 395.
 Dressler, A., Lynden-Bell, D., Burstein, D., Davies, R., Faber, S., Terlevich, R., and Wegner, G. 1987, Ap. J., 313, 42.
 Ferguson, H.C., and Sandage, A. 1988, A. J., 96, 1520.
 Hanes, D.A., and Harris, W.E. 1986, Ap. J., 309, 564.
 Hanes, D.A., and Whittaker, D.G. 1987, A. J., 94, 906.
 Harris, H.C., and Canterna, R. 1977, A. J., 82, 798.
 Harris, H.C., and Canterna, R. 1979, A. J., 84, 1750.
 Harris, W.E. 1987, Publ. A.S.P., 99, 1031.
 Harris, W.E. 1989, "The Extragalactic Distance Scale," A.S.P. Conf. Series, Vol. 4, ed. S. van den Bergh and C.J. Pritchett, p. 231.
 Harris, W.E., and Smith, M.G. 1976, Ap. J., 207, 1036.
 Harris, W.E., Smith, M.G., and Myra, E.S. 1983, Ap. J., 272, 456.
 Hesser, J.E., and Shawl, S.J. 1985, Publ. A.S.P., 97, 465.
 Jones, R.V., Carney, B.W., Latham, D.W., and Kurucz, R.L. 1987, Ap. J., 314, 605.
 Mould, J.R., Oke, J.B., and Nemec, J.M. 1987, A. J., 93, 53.
 Reed, B.C., Hesser, J.E., and Shawl, S.J. 1988, Publ. A.S.P., 100, 545.
 Stetson, , P.B. 1987, Publ. A.S.P., 99, 191.
 Zinn, R. 1980, Ap. J. Suppl., 42, 19.
 Zinn, R. 1985, Ap. J., 293, 424.

Doug Geisler: National Optical Astronomy Observatories, Cerro Tololo Inter-american Observatory, Casilla 603, La Serena, Chile.

Juan Carlos Forte: Instituto de Astronomía y Física del Espacio, Casilla de Correo 67, Sucursal 28, 1428, Buenos Aires, Argentina.